INTERNATIONAL JOURNAL OF ELECTRONICS
https://doi.org/10.1080/00207217.2019.1608588

Angle estimation in MIMO radar using a new sparse representation approach

Baobao Liu[a], Ercan Engin. Kuruoglu[b], Junying Zhang[c], Fulvio Gini[d], Tao Xue[a] and Wenying Lei[e]

[a]School of Computer Science, Xi'an Polytechnic University, Xi'an, China; [b]Istituto di Scienza e Tecnologie dell'Informazione, ''A. Faedo'', CNR, Pisa, Italy; [c]School of Computer Science and Technology, Xidian University, Xi'an, China; [d]Dipartimento di Ingegneria dell'Informazione, University of Pisa, Pisa, Italy; [e]China Academy of Space Technology, Beijing, China

ABSTRACT

Existing direction of arrival (DOA) estimation methods in multiple-input multiple-out (MIMO) radar systems will encounter the performance degradation in the cases of few snapshots, low signal-to-noise ratio (SNR), closely spaced targets, or strongly correlated sources. To improve it, this paper develops a new sparse representation-based DOA estimation method. The main contributions are as follows: i) we construct a new real-valued double weighted $l_{2,1}$-norm minimisation model; ii) we derive an improved reduced-dimension technique to enhance estimation accuracy; and iii) we design optimal and sparse weights carefully to improve the corresponding estimation accuracy. Finally, the effectiveness and theoretical analysis of the presented approach are verified by extensive numerical simulations, which proves that the new algorithm performs well at low SNR and with a small number of snapshots as well as at the coherent source case.

ARTICLE HISTORY
Received 27 September 2018
Accepted 6 April 2019

KEYWORDS
Multiple-input multiple-output radar; direction of arrival (DOA); unitary transformation; sparse representation; subspace fitting

1. Introduction

Multiple-input multiple-output (MIMO) radar exploits multiple transmitters to simultaneously propagate diverse waveforms and thus uses multiple receivers to receive the reflected signals from targets (Haimovich, Blum, Chizhik, Ciminim, & Valenzuela, 2004). It received a lot of attentions (Chen, Chen, & Qian, 2008; Chen, Gu, & Su, 2008; Gao, Zhang, Feng, Wang, & Xu, 2009, Haimovich, Blum, & Cimini, 2008; Hassanien & Vorobyov, 2011; Li & Li, 2012; Li & Stoic, 2007) owing to the potential advantages of MIMO radar such as powerful sensitivity beneficial to detect slowly moving targets, better parameter identifiability, more degree of freedom (DOF) and better angular resolution over conventional phased-array radar (Haimovich et al., 2004, 2008; Li & Stoic, 2007). Generally, according to the configuration of the transmitting array and receiving array, MIMO radar can be divided into two types. One is called statistical MIMO radar, whose transmitting elements and receiving elements are widely spaced. Another is called co-located MIMO radar (Li & Stoic, 2007) including monostatic MIMO radar and bistatic MIMO radar, in which transmitting elements and receiving elements are closely spaced.

CONTACT Baobao Liu liubaobao1222@163.com School of Computer Science, Xi'an Polytechnic University, Xi'an 710048, China

The co-located MIMO radar can acquire unambiguous angle estimation since it can provide virtual beneficial aperture, which is bigger than real aperture. In this paper, we focus on monostatic co-located MIMO radar for direction of arrival (DOA) estimation of multiple targets, which is one of most significant aspects in array signal processing fields (Chen et al., 2008, 2008; Gao et al., 2009; Hassanien & Vorobyov, 2011; Li & Li, 2012).

Recently, several algorithms have been proposed for DOA estimation in MIMO radar (Chen et al., 2008, 2008; Gao et al., 2009; Hassanien & Vorobyov, 2011; Li & Li, 2012). In (Li & Li, 2012), a low complexity Capon-based algorithm is developed for monostatic radar, which is of lower complexity and has higher estimation performance than those of the common Capon algorithm. In (Gao et al., 2009), a multiple signal classification algorithm is exploited, however, it is computationally expensive resulted from peak search. (Chen et al., 2008, 2008) present several estimations of signal parameters via rotational invariance technique (ESPRIT) algorithms, which utilise the rotational invariance property of both the transmitting and receiving arrays and thus have low computational cost as they need not search spectral peaks. In (Hassanien & Vorobyov, 2011), a transmitting beamspace energy focusing approach is designed, and angle estimation performance is enhanced as transmitting beamspace weight matrix with the SNR gain is maximised for each receive antenna. However, all these methods consider only non-correlated source environments. Additionally, they mentioned above hinge on target priori information and high accurate covariance matrix estimation, and their angle estimation performance decreases greatly in the situation of low signal-to-noise ratio (SNR), limited snapshots and closely spaced targets. In other words, they can obtain beneficial angle estimation accuracy, provided that the targets are not strongly correlated, the number of snapshots is sufficient, the targets are not close to each other, or the SNR is high enough. They still can not work well under the coherent source case. Hence, it is time that we should develop a beneficial angle estimation algorithm to tackle the problems of the existing algorithms in MIMO radar.

More recently, sparse representation has attracted a great deal of attention for DOA estimation in array signal processing (Hu, Ye, Xu, & Cao, 2012; Hyder & Mahata, 2008; Liu, Huang, & Zhou, 2013; Malioutov, Cetin, & Willsky, 2005; Steffens & Pesavento, 2018; Wang, Huang, & Zhang, 2011; Yin & Chen, 2011; Zhen, Li, Liu, & Wang, 2012; Zheng, Li, & Wang, 2013). In (Malioutov et al., 2005), l_1-norm singular value decomposition (l_1-SVD) algorithm is developed for DOA estimation via using sparse recovery, which has several advantages over conventional source localisation techniques such as high resolution, robustness to noise and correlation of signals. Literature (Liu et al., 2013) derives a sparse representation of covariance matrix approach, which can estimate both the number and directions of targets via sparsely representing a vector constructed with array output matrix elements. In (Yin & Chen, 2011), a sparse representation of array covariance vector (SRACV) algorithm is developed to estimate both coherent and uncorrelated sources for an arbitrary configuration of array, which has high angle estimation accuracy. In (Hyder & Mahata, 2008), a sparse recovery iterative algorithm is proposed for the single measurement vector (SMV) case. In (Hu et al., 2012), a sparse subspace fitting algorithm is introduced. In (Zhen et al., 2012), a sparse representation angle estimation algorithm is presented by combining unitary transformation with the weighted l_1-norm sparsity signal recovery method. However, MIMO radar angle estimation generally encounters with multiple measurement vector (MMV) problem, and the iterative algorithm may not be exploited to estimate angle. Furthermore, the two-dimensional dictionary matrix is constructed for recovering sparse signal matrix in MIMO radar, which causes very heavy computational burden owing to complex-valued process and MMV problem. Hence, the above-mentioned sparse algorithms are extended difficulty to DOA estimation for MIMO radar owing to high computational cost. Furthermore, these techniques (Hu et al., 2012; Hyder & Mahata, 2008; Liu et al., 2013; Malioutov et al., 2005; Wang et al., 2011; Yin & Chen, 2011; Zhen et al., 2012; Zheng et al., 2013) concern only angle estimation for conventional radar, which are seldom exploited to address the DOA estimation in MIMO radar (Qian, He, & Zhang, 2018).

To tackle these challenging problems, and inspired by the sparse representation l_1-SVD algorithm (Malioutov et al., 2005) and the subspace fitting method (Hu et al., 2012; Zhen et al., 2012) in array signal processing, we design a new sparse representation approach via constructing a real-valued double weighted $l_{2,1}$-norm minimisation model for DOA estimation in monostatic MIMO radar. In the presented method, an improved reduced-dimension technique is utilised to transform the high dimensional complex-valued received data into low dimensional one. Secondly, the low dimensional data are transformed into a low dimensional real-valued data by employing a unitary transformation technique, thereby diminishing computational complexity. Thirdly, the optimal and sparse weights are devised to enhance estimation accuracy since the reduced computational cost techniques lead to slight angle estimation performance degradation. Thus, the real-valued double weighted $l_{2,1}$-norm minimisation model is formulated for DOA estimation when multiple snapshots are available. The simulation results prove that the proposed methodology can acquire high angle estimation accuracy, improved angular separation performance and low sensitivity to the assumed number of targets in comparison with RD-ESPRIT (Zhang & Xu, 2011) and RD-Capon algorithms (Li & Li, 2012), especially in relatively small number of snapshots and/or low SNR and closely spaced targets case. Furthermore, the proposed algorithm works well under coherent source environments. To the best of our knowledge, no similar sparse representation methodology has been investigated yet so far for angle estimation in monostatic MIMO radar. The major contributions of the paper as follows:

(1) Derive an improved reduced-dimension technique to enhance estimation accuracy of the new algorithm.
(2) By employing a unitary transformation technique, the low dimensional complex-valued received data are transformed into a low dimensional real-valued data, thereby diminishing computational complexity. The optimal and sparse weights are designed carefully to improve the corresponding angle estimation performance.
(3) Propose a new sparse representation approach by constructing a real-valued double weighted $l_{2,1}$-norm minimisation model.

The remainder of the paper is organised as follows. Section 2 introduces the monostatic radar signal model. Section 3 demonstrates the proposed algorithm for DOA estimation in monostatic radar. Section 4 provides computational complexity of the proposed algorithm and CRB. Section 5 shows the extensive simulation results. Finally, conclusions are summarised in Section 6

Notation: $(\cdot)^H$ and $(\cdot)^{-1}$ signify conjugate transpose and inverse operations, respectively. $\mathrm{Re}(\cdot)$ is to obtain the real part of the complex value. $\otimes$ and $\oplus$ denote Kronecker and Handamard product, respectively. I_{MN} is an $MN \times MN$ identity matrix. $\|\cdot\|_F$ and $\|\cdot\|_1$ signify Frobenius norm and the l_1 norm, respectively. $diag(v)$ denotes diagonal matrix whose diagonal is a vector. $E(.)$ represents expectation operator.

2. Signal model

Without loss of generality, we consider a narrowband monostatic MIMO radar system composed of M transmitting elements and N receiving elements, both of which are half-wavelength spaced uniform linear arrays (Chen et al., 2008, 2008; Gao et al., 2009; Hassanien & Vorobyov, 2011; Li & Li, 2012), as shown in Figure 1. In the transmitting array, M different narrowband orthogonal waveforms are transmitted simultaneously by M transmitting antennas, which have identical bandwidth and centre frequency. Suppose that P signifies the number of uncorrelated targets, and the DOA of the *pth* target is denoted by θ_p with respect to the normal of transmitting and receiving arrays. Then, the output of the matched filter in the receiving array can be formulated as (Chen et al., 2008, 2008; Gao et al., 2009; Hassanien & Vorobyov, 2011; Li & Li, 2012)

$$\mathbf{x}(t) = [\mathbf{a}_r(\theta_1) \otimes \mathbf{a}_t(\theta_1), \ldots, \mathbf{a}_r(\theta_p) \otimes \mathbf{a}_t(\theta_p)]\mathbf{s}(t) + \mathbf{n}(t) \tag{1}$$

where $\mathbf{s}(t) = [s_1(t), s_2(t), \ldots, s_P(t)]^T \in \mathbb{C}^{P\times 1}$ and $s_p(t) = \alpha_p e^{j2\pi f_p t}$ with α_p being the amplitude and f_p Doppler frequency. $\mathbf{a}_r(\theta_p)$ and $\mathbf{a}_t(\theta_p)$ denote the receive steering vector and transmit steering vector for θ_p, respectively; $\mathbf{a}_r(\theta_p) \otimes \mathbf{a}_t(\theta_p)$ signifies the Kronecker product. $\mathbf{a}_r(\theta_p) = [1, \exp(-j\pi \sin\theta_p), \ \ldots, \exp(-j\pi(N-1)\sin\theta_p)]^T, \ldots, \mathbf{a}_t(\theta_p) = [1, \exp(-j\pi \sin\theta_p), \exp(-j\pi(M-1)\sin\theta_p)]^T$. $\mathbf{n}(t)$ signifies an $MN \times 1$ Gaussian white noise vector with zeros mean and covariance matrix $\sigma^2\mathbf{I}_{MN}$. We define $\mathbf{A} = [\mathbf{a}_r(\theta_1) \otimes \mathbf{a}_t(\theta_1), \ldots, \mathbf{a}_r(\theta_p) \otimes \mathbf{a}_t(\theta_p)]$; then, the received data in Equation (1) can be rewritten as $\mathbf{x}(t) = \mathbf{A}\mathbf{s}(t) + \mathbf{n}(t)$. In the case of multiple snapshots, we collect L snapshots and the received data can be expressed as

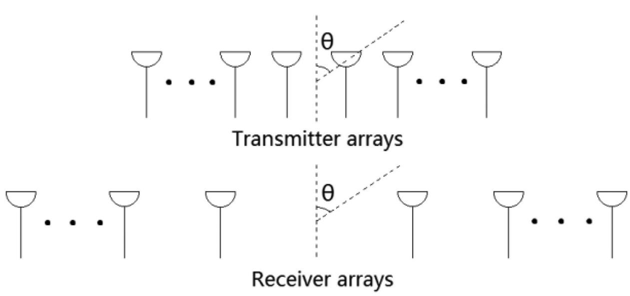

Figure 1. The monostatic MIMO radar configuration.

$$\mathbf{X} = \mathbf{AS} + \mathbf{N} \tag{2}$$

where $\mathbf{X} = [\mathbf{x}(t_1), \ldots, \mathbf{x}(t_L)]$, $\mathbf{S} = [\mathbf{s}(t_1), \ldots, \mathbf{s}(t_L)]$ and $\mathbf{N} = [\mathbf{n}(t_1), \ldots, \mathbf{n}(t_L)]$ is the Gaussian white noise matrix.

3. New sparse representation approach for DOA estimation

In this section, we first employ the improved reduced-dimension technique to transform the high dimensional complex-valued received data into low dimensional one. Secondly, we exploit the unitary transformation technique to transform the low dimensional data into a low dimensional real-valued data. Thirdly, we devised the optimal and sparse weights to enhance the angle estimation. Finally, the real-valued double weighted $l_{2,1}$-norm minimisation model is formulated for DOA estimation.

3.1 Reduced-dimension transformation for received data

It has been mentioned above that the sparse presentation approaches are extended difficulty to DOA estimation for MIMO radar owing to high computational cost. Thus, we first employ an improved reduced-dimension technique transform the high dimensional complex-valued received data into low dimensional one. Referring to (Li & Li, 2012; Xie, Liu, & Zhang, 2010; Xu, Li, & Stocia, 2006), it is evident that the transmit-receive steering vector has only $(M + N - 1)$ distinct elements. Thus, $\mathbf{a}_r(\theta_p) \otimes \mathbf{a}_t(\theta_p)$ can be given by

$$\mathbf{a}_r(\theta_p) \otimes \mathbf{a}_t(\theta_p) = \mathbf{G}\mathbf{b}(\theta_p) \tag{3}$$

where $\mathbf{b}(\theta_p) = [1, \exp(-j\pi \sin\theta_p), \ldots, \exp(-j\pi(M + N - 2)\sin\theta_p)]^T$ is the $(M + N - 1) \times 1$ Vand-ermonde vector which relies on θ and M, and $\mathbf{G}$ is the $MN \times (M + N - 1)$ transformed matrix as follows:

$$\mathbf{G} = \left[\begin{array}{l} \left.\begin{matrix} 1 & 0 & \cdots & 0 & 0 & \cdots & 0 \\ 0 & 1 & \cdots & 0 & 0 & \cdots & 0 \\ \vdots & \vdots & \ddots & \vdots & \vdots & \ddots & \vdots \\ 0 & 0 & \cdots & 1 & 0 & \cdots & 0 \end{matrix}\right\} M \\ \left.\begin{matrix} 0 & 1 & \cdots & 0 & 0 & \cdots & 0 \\ 0 & 0 & 1 & 0 & 0 & \cdots & 0 \\ \vdots & \vdots & \vdots & \ddots & \vdots & \ddots & \vdots \\ 0 & 0 & \cdots & 0 & 1 & \cdots & 0 \end{matrix}\right\} M \\ \cdots \\ \cdots \\ \left.\begin{matrix} 0 & \cdots & 0 & 1 & 0 & \cdots & 0 \\ 0 & \cdots & 0 & 0 & 1 & \cdots & 0 \\ \vdots & \cdots & \vdots & \cdots & \vdots & \ddots & \vdots \\ 0 & \cdots & 0 & 0 & 0 & \cdots & 1 \end{matrix}\right\} M \end{array}\right] \in C^{MN \times (M+N-1)} \tag{4}$$

According to Equation (4), we let be $\mathbf{F} = \mathbf{G}^H\mathbf{G}$, which is further presented as

$$\mathbf{F} = diag[1, 2, \ldots, \underbrace{\min(M, N), \ldots, \min(M, N)}_{|M-N|+1}, \ldots, 2, 1] \tag{5}$$

In order to whiten coloured noise, we define the reduced-dimension transformation matrix $\mathbf{D}$ as

$$\mathbf{D} = \mathbf{F}^{-(1/2)}\mathbf{G}^H \tag{6}$$

Applying the reduced-dimension transformation $\mathbf{F}^{-(1/2)}\mathbf{G}^H$ for the received signal $\mathbf{x}(t)$, we have

$$\begin{aligned} \mathbf{y}(t) &= \mathbf{F}^{-(1/2)}\mathbf{G}^H\mathbf{x}(t) \\ &= \mathbf{F}^{-(1/2)}\mathbf{F}[\mathbf{b}(\theta_1), \mathbf{b}(\theta_2), \ldots, \mathbf{b}(\theta_P)]\mathbf{s}(t) + \mathbf{F}^{-(1/2)}\mathbf{G}^H\mathbf{n}(t) \\ &= \mathbf{F}^{(1/2)}\mathbf{B}\mathbf{s}(t) + \mathbf{F}^{-(1/2)}\mathbf{G}^H\mathbf{n}(t) \end{aligned} \tag{7}$$

where $\mathbf{B} = [\mathbf{b}(\theta_1), \mathbf{b}(\theta_2), ..., \mathbf{b}(\theta_P)]$. Till now, the low dimensional received data $\mathbf{y}(t)$ is obtained. The covariance matrix of the noise in (7) is shown as follows (Li & Li, 2012):

$$\bar{\mathbf{R}}_n = \mathbf{E}[\mathbf{F}^{-(1/2)}\mathbf{G}^H\mathbf{n}(t)(\mathbf{F}^{-(1/2)}\mathbf{G}^H\mathbf{n}(t))^H] = \mathbf{F}^{-(1/2)}\mathbf{G}^H\mathbf{E}[\mathbf{n}(t)\mathbf{n}^H(t)]\mathbf{G}^H\mathbf{F}^{-(1/2)} \tag{8}$$

Although the reduced-dimension transformation technique does not lead to additional colouring (Li & Li, 2012), we can see from Equation (7) that the signal part contains amplitude error $\mathbf{F}^{(1/2)}$, which is difficult to be calibrated by conventional calibration methods and can significantly impact angle estimation performance of the existing algorithms based on reduced-dimension transformation especially in relatively small number of snapshots and/or low SNR. In the following components, we introduce how to calibrate amplitude error step by step. The reduced-dimension signal covariance matrix is then given by

$$\begin{aligned} \mathbf{R}_y &= \mathbf{E}[\mathbf{y}(t)\mathbf{y}^H(t)] = \mathbf{F}^{1/2}\mathbf{B}[s(t)s^H(t)]\mathbf{B}^H\mathbf{F}^{1/2} + \sigma^2\mathbf{I}_{M+N-1} \\ &= \mathbf{U}_{so}\mathbf{\Lambda}_{so}\mathbf{U}_{so}^H + \mathbf{U}_n\mathbf{\Lambda}_n\mathbf{U}_n^H \end{aligned} \tag{9}$$

where $\mathbf{\Lambda}_{so}$ is a diagonal matrix, the columns of $\mathbf{U}_{so}$ are the eigenvectors corresponding to the P largest eigenvalues, while the columns of $\mathbf{U}_n$ are the eigenvectors corresponding to $M + N - 1 - P$ smallest eigenvalues. The $\mathbf{F}^{1/2}\mathbf{B}$ contains amplitude error $\mathbf{F}^{1/2}$, which is manifested on the rows of $\mathbf{\Lambda}_{so}^{1/2}$. Then, we define $\bar{\mathbf{R}}_y = \mathbf{B}[\mathbf{s}(t)\mathbf{s}^H(t)]\mathbf{B}^H = \mathbf{F}^{-(1/2)}\mathbf{U}_{so}\mathbf{\Lambda}_{so}\mathbf{U}_{so}^H\mathbf{F}^{-(1/2)}$ and we can obtain P-snapshot signal matrix $\mathbf{S}_o = \mathbf{F}^{-(1/2)}\mathbf{U}_{so}\mathbf{\Lambda}_{so}^{1/2}$. Then, the amplitude error $\mathbf{F}^{(1/2)}$ including $\mathbf{\Lambda}_{so}^{1/2}$ is compensated by using $\mathbf{F}^{(-1/2)}$. $\mathbf{S}_o$ can be represented as $\mathbf{S}_o = \mathbf{BT}$, where $P \times P$ -dimensional matrix $\mathbf{T}$ is full-rank. In practice,

$\mathbf{\Lambda}_{so}^{1/2}$ always has noise components. The optimal $\mathbf{\Lambda}_s$ is obtained by solving Equation (10)

$$\min_{\mathbf{\Lambda}_s, \mathbf{T}_1} \left\| \mathbf{U}_{so}\mathbf{\Lambda}_s^{1/2} - \mathbf{F}^{1/2}\mathbf{B}\mathbf{T}_1 \right\|_F^2 \tag{10}$$

then, the optimal solution can be represented as $\mathbf{\Lambda}_s = (\mathbf{\Lambda}_{so} - \sigma_o^2\mathbf{I}_P)^2\mathbf{\Lambda}_{so}^{-1}$ according to the references (Harry, 2002; Viberg & Ottersten, 1991; Viberg, Ottersten, & Kailath, 1991), where $\sigma_o^2 = \frac{1}{M+N-1-P}\sum_{i=P+1}^{M+N-1}\lambda_i, \; i = P+1, \ldots, M+N-1$. Eventually, we can obtain P-snapshots data matrix $\mathbf{S}_1 = \mathbf{F}^{-(1/2)}\mathbf{U}_{so}\mathbf{\Lambda}_s^{1/2} \in \mathbb{C}^{(M+N-1)\times P}$, which do not have amplitude error.

Remark 1: The proposed algorithm not only provides low computational cost but also has high estimation accuracy by using the reduced-dimension method without causing amplitude error in comparison with previous reduced-dimension method (Li & Li, 2012; Xie et al., 2010; Xu et al., 2006).

3.2 Unitary transformation for low dimensional received data

In this section, the low dimensional P-snapshot data matrix $\mathbf{S}_1$ is transformed into to a centro-Hermitian matrix $\mathbf{Z}$ that composes the spatial smoothing technique (Haardt & Nossek, 1995) as follows:

$$\mathbf{Z} = \left[\mathbf{S}_1,\ \mathbf{\Pi}_{M+N-1}\mathbf{S}_1{}^*\mathbf{\Pi}_P\right] \tag{11}$$

where $\mathbf{\Pi}_{M+N-1}$ signifies the exchange matrix with ones on its anti-diagonal and zeros elsewhere and $(\cdot)^*$ represents the complex conjugate. Then, the low dimensional real-valued extended data matrix $\mathbf{\Gamma}$ is constructed by applying unitary transformation on the complex-valued extended data matrix $\mathbf{Z}$ as follows (Haardt & Nossek, 1995; Huarng & Yeh, 1991; Thakre, Haardt, & Giridhar, 2009)

$$\mathbf{\Gamma} = \mathbf{Q}^H_{M+N-1}\mathbf{Z}\mathbf{Q}_{2P} = \mathbf{Q}^H_{M+N-1}\left[\mathbf{Y},\ \mathbf{\Pi}_{M+N-1}\mathbf{S}_1{}^*\mathbf{\Pi}_P\right]\mathbf{Q}_{2P} \in R^{(M+N-1)\times 2P} \tag{12}$$

where $(\cdot)^H$ represents the complex conjugate transpose, and $\mathbf{Q}$ is defined for even and odd order, respectively, which is the unitary transformation matrix, can be expressed as

$$\mathbf{Q}_P = \frac{1}{\sqrt{2}}\begin{bmatrix} \mathbf{I}_P & j\mathbf{I}_P \\ \mathbf{\Pi}_P & -j\mathbf{\Pi}_P \end{bmatrix},\ \mathbf{Q}_{2P+1} = \frac{1}{\sqrt{2}}\begin{bmatrix} \mathbf{I}_P & 0 & j\mathbf{I}_P \\ \mathbf{0}^T & \sqrt{2} & \mathbf{0}^T \\ \mathbf{\Pi}_P & 0 & -j\mathbf{\Pi}_P \end{bmatrix} \tag{13}$$

where $\mathbf{\Gamma} \in \mathbf{R}^{(M+N-1)\times 2P}$ is in real domain after implementing the unitary transformation, then, a low dimensional real-valued covariance matrix can be estimated as follows:

$$\hat{\mathbf{R}}_{real} = \frac{1}{2P}\mathbf{\Gamma}\mathbf{\Gamma}^H \tag{14}$$

and we can find from Equation (12) that the number of snapshots is doubled, which can further enhance the jointly sparse constraint. Then, implement the singular value decomposition (SVD) on low dimensional real-valued matrix $\hat{\mathbf{R}}_{real}$, and the real-valued signal subspace $\mathbf{U}_s$ and the real-valued noise subspace $\mathbf{U}_n$ can be obtained, respectively, according to the magnitude of corresponding singular values.

Remark 2. In the presented method, a unitary transformation technique is exploited to double the number of data samples, which can further boost the jointly sparse constraint on the solution, suppress spurious peaks, enhance angle estimation performance, improve decorrelation ability for the unitary technique implies spatial smoothing method (Haardt & Nossek, 1995). Furthermore, the low dimension complex-valued received data is transformed into a real-valued data, thereby diminishing computational complexity.

3.3 Angle estimation in monostatic MIMO radar

In this section, sparse weights are devised to enhance estimation accuracy since we exploit the improved reduced-dimension technique lead to slight angle estimation performance degradation. To describe the sparse weighting idea briefly, let

$$\widehat{\mathbf{W}} = (\mathbf{Q}_{M+N-1}^H \mathbf{\Phi})^H \mathbf{U}_n = \mathbf{\Phi}^H \mathbf{Q}_{M+N-1} \mathbf{U}_n \tag{15}$$

then, by exploiting the orthogonality between the noise subspace and the array manifold matrix, the $\widehat{\mathbf{W}}$ is rewritten as follows (Zhen et al., 2012):

$$\widehat{\mathbf{W}} = \begin{bmatrix} \mathbf{\Phi}_{\Lambda}^H \mathbf{Q}_{M+N-1} \mathbf{U}_n \\ \mathbf{\Phi}_{\Lambda^c}^H \mathbf{Q}_{M+N-1} \mathbf{U}_n \end{bmatrix} \tag{16}$$

where Λ^c represents the complementary of setting to Λ.

Remark 3. As the proof of the sparse weighting has been given in Ref. (Zhen et al., 2012; Zheng et al., 2013) for angle estimation in conventional radar, and also owing to page limitation, here, the detailed discussion of this problem is omitted. In this paper, we extend the sparse weighting scheme to the proposed algorithm for angle estimation in monostatic MIMO radar.

Then, define $\Theta = \left\{\widehat{\theta}_1, \widehat{\theta}_2, \ldots \widehat{\theta}_D\right\}$ as a dense sampling grid of all DOAs of interest and assume that the true DOAs belong to Θ. An $(M+N-1) \times D$ overcomplete basis matrix $\mathbf{\Phi} = [\mathbf{b}(\widehat{\theta}_1), \mathbf{b}(\widehat{\theta}_2), \ldots, \mathbf{b}(\widehat{\theta}_D)]$ is given by employing Θ. Then, combining the sparse representation technique and subspace fitting scheme (Hu et al., 2012; Viberg & Ottersten, 1991; Viberg et al., 1991; Zhen et al., 2012), the real-valued sparse representation framework in monostatic MIMO radar is given by

$$\mathbf{U}_s \mathbf{W}_{opt}^{1/2} = \mathbf{Q}_{M+N-1}^H \mathbf{\Phi} \tilde{S} + \mathbf{E} \tag{17}$$

where complex-valued overcomplete basis marix $\mathbf{\Phi}$ is transformed into real-valued overcomplete baise marix by using $\mathbf{Q}_{M+N-1}^H$. $\mathbf{E}$ is a real-valued Gaussian noise. $\tilde{S}$ has a few non-zero rows and its the *ith* row corresponds to DOAs of the possible. Thus, $\tilde{S}$ is a sparse spatial spectrum. In order to recover the sparse matrix $\tilde{S}$, we consider the real-valued double weighted $l_{2,1}$-norm constrained minimisation problem as follows:

$$\min \|\tilde{S}\|_{\bar{w};2,1}, \; s.t \left\| \mathbf{U}_s \mathbf{W}_{opt}^{1/2} - \mathbf{Q}_{M+N-1}^H \mathbf{\Phi} \tilde{S} \right\|_F^2 \leq \beta^2 \tag{18}$$

where $\|.\|_{\widehat{w};2,1} \triangleq \sum_{d=1}^{D} \widehat{w}_d (\sum_{p=1}^{P} |[.]_{d.p}|^2)^{1/2}$ and $\mathbf{W}_{opt} = (\mathbf{\Lambda}_s - \sigma^2 \mathbf{I}_P)^2 \mathbf{\Lambda}_s^{-1}$, $\mathbf{\Lambda}_s$ is a diagonal matrix and σ^2 is noise variance. For detailed knowledge of the optimal weight $\mathbf{W}_{opt}$ is already presented in ref. (Harry, 2002; Viberg & Ottersten, 1991; Viberg et al., 1991) and also detailed discussion of this subject referring in (Harry, 2002; Viberg & Ottersten, 1991; Viberg et al., 1991). β^2 is a regulation parameter which can be given by a χ^2 distribution with $(M+N-1) \times P$ degrees of freedom and 0.99 probability (Malioutov et al., 2005). The DOAs can be estimated by finding the nonzero elements of $\tilde{S}^{(l_2)}$ by solving $\tilde{S}^{(l_2)}$. Here, the second-order cone (SOC) problem in Equation (18) can be solved by exploiting CVX package (Grant & Boyd). Then, we can estimate DOA in monostatic MIMO radar by plotting $\tilde{S}^{(l_2)}$, solved from Equation (18).

4. Computational complexity analysis and the Cramér-Rao Bound (CRB)

The main computational complexity of the proposed algorithm is $o\{(M+N-1)^2+2(M+N-1)^3+2(M+N+2P)+(M+N-1)^3P^3\}$. The RD-Capon and RD-ESPRIT computational complexity are $o\left\{(M+N-1)^2L+(M+N-1)^3+L[(M+N)(M+N-1-P)]\right\}$ and $o\left\{(M+N-1)^2L+(M+N-1)^3\right\}$, respectively. Even though the proposed algorithm utilises the reduced-dimension technique, the real-valued processing method and SVD method to decrease the computation complexity of sparse signal reconstruction, the computation complexity of the proposed algorithm is higher than the RD-Capon and RD-ESPRIT algorithms. However, the advantages of the proposed algorithm outweigh the cost of additional computation: the presented algorithm obtains high angle estimation accuracy, beneficial angular separation performance, low sensitivity to the assumed number of targets, and works well coherent source environments without requiring the decorrelation procedure. Furthermore, according to (Li & Li, 2012; Stoica & Nehorai, 1990), the CRB of angle estimation is given by

$$\mathbf{CRB}=\frac{\sigma^2}{2L}\left\{\mathbf{Re}\left[\left(\mathbf{D}^H\mathbf{\Pi}_{\mathbf{A}}^{\perp}\mathbf{D}\right)\oplus\widehat{\mathbf{R}}^T\right]\right\}^{-1} \tag{19}$$

where $\oplus$ signifies the Hadamard product, $\mathbf{\Pi}_{\mathbf{A}}^{\perp}=\mathbf{I}_{MN}-\mathbf{A}(\mathbf{A}^H\mathbf{A})^{-1}\mathbf{A}^H$, $\widehat{\mathbf{R}}=\frac{1}{L}\sum_{l=1}^{L}s(t_l)s^H(t_l)$, $\mathbf{D}=[\mathbf{h}_1,\mathbf{h}_2,\ldots,\mathbf{h}_P]$, $\mathbf{h}_p=\partial(\mathbf{a}_r(\theta_p)\otimes\mathbf{a}_t(\theta_p))/\partial\theta_p$.

The presented algorithm has the following advantages:

(1) It can perform well in the cases of the strongly correlated and coherent source environments.
(2) It can work well in the situation of a small number of snapshots and/or low SNR and closely spaced targets case.
(3) It has much better angle estimation accuracy than that of the RD-Capon algorithm (Li & Li, 2012) and RD-ESPRIT, which will be shown in the following section.
(4) It has a low sensitivity to the assumed number of targets.

5. Simulation results

In this section, we demonstrate the superiority of the proposed algorithm over existing algorithms, including the RD-ESPRIT (Zhang & Xu, 2011) and RD-Capon algorithms (Li & Li, 2012), by the extensive numerical examples. The root mean squared error (RMSE) of evaluation angle estimation performance is defined as

$$\text{RMSE} = \sqrt{\frac{1}{(PK)}\sum_{p=1}^{P}\sum_{k=1}^{K}\left(\hat{\theta}_{p,k} - \theta_p\right)^2} \tag{20}$$

where $\hat{\theta}_{p,k}$ is the estimation of θ_p of the kth Monte Carlo trial. In the following simulation examples, 200 Monte Carlo trials are exploited, and the spatial direction grid is uniform with 0.1° sampling between -90° with 90°. We assume that there are three uncorrelated targets, which are located at angles $\theta_1 = 10.5^\circ$, $\theta_2 = 20.7^\circ, \theta_3 = 30.8^\circ$, respectively.

Figure 2 describes the spatial spectra of the proposed algorithm and RD-Capon for three uncorrelated targets with $M = 8$, $N = 8$, $L = 300$, and SNR $= 10$ dB. We can see from Figure 2(a) that our technique obtains more sharp peaks than that of RD-Capon since we exploit the optimal and sparse weights, and the unitary transformation technique to enhance estimation performance of the proposed algorithm. Furthermore, as we can see from Figure 2(b), the proposed algorithm can distinguish closely targets effectively while the RD-Capon fails to the work.

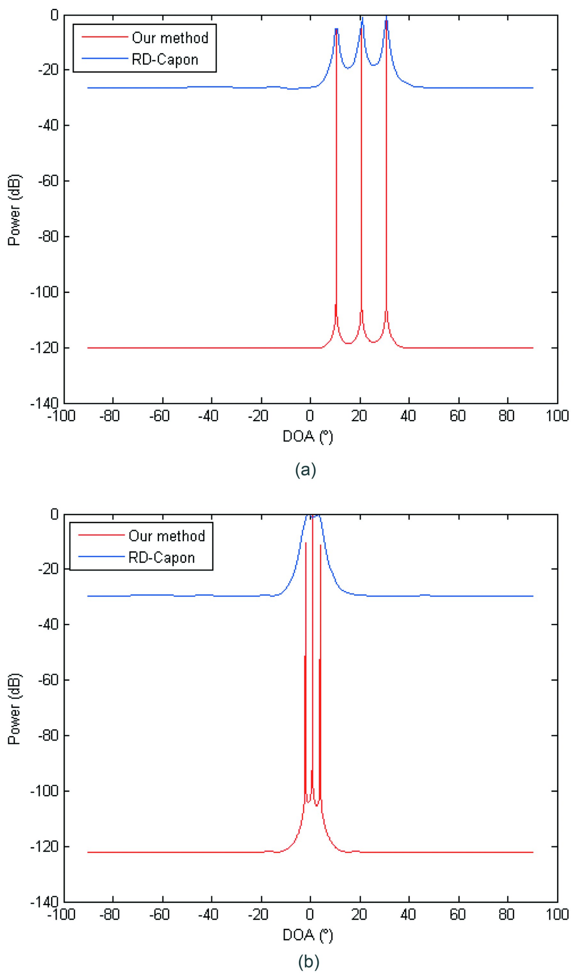

Figure 2. (a) Spatial spectra comparison with three uncorrelated targets. (b) Spatial spectra comparison three uncorrelated targets. DOAs: -2°, 1°, 4°.

Table 1. Angle estimation of results of the RD-ESPRIT.

$\theta_1 = 4^\circ$	$\theta_1 = 1^\circ$	$\theta_1 = -2^\circ$
3.8104	1.1322	−2.2271
3.8967	1.1602	−1.8320
3.9747	1.2618	−2.0982
4.0337	0.6552	−2.0711
3.9675	0.7232	−2.2099

Table 1. shows that the angle estimation of results of the RD-ESPRIT for three uncorrelated targets with M = 8, N = 8, L = 200, and SNR = 10 dB. It can be seen from Table 1 that the RD-ESPRIT method can also effectively distinguish closely targets. From Figures 5 and 6, we can observe that the proposed method estimation accuracy better than the RD-ESPRIT.

Figure 3 presents the angle estimation of results of the proposed algorithm and RD-Capon for three coherent targets with $M = 8$, $N = 8$, and SNR = 10 dB. As we can see from Figure 3, the proposed algorithm can effectively estimate coherent targets, which does not require decorrelation procedure while the RD-Capon fails to the work. On the other hand, Figure 3 further demonstrates that our technique can obtain spatial smoothing (Haardt & Nossek, 1995; Harry, 2002; Huarng & Yeh, 1991) ability by unitary transformation and angle estimation performance of our technique is effectively boosted in contrast to the Capon algorithm.

In this simulation, we indicate the sensitivity of our technique to the priori information of the target number in Figure 4, where $M = 8$, $N = 8$, $L = 300$, and SNR = 10 dB are adopted. As we can see from Figure 4, the proposed algorithm can correctly estimate the number of targets, which has low sensitivity that affords beneficial robustness against mistakes in estimating the number of targets. The main reason is that sparse weighting does not depend on the priori information of the target number. Moreover, the unitary transformation technique promotes sparsity and thus the proposed algorithm obtains more accurate angle estimation.

Figure 5 illustrates angle estimation performance comparison, where we compare the proposed algorithm with the RD-Capon and RD-ESPRIT algorithms. Then, it can be clearly seen from Figure 5 that the proposed algorithm has lower RMSE than that of RD-Capon and RD-ESPRIT algorithms, especially in the low SNR case. The RMSE of the proposed algorithm approaches to the CRB since we adopt the optimal and sparsity weights, and the unitary transformation technique to improve estimation performance of the proposed algorithm. Thus, the proposed algorithm enjoys superior angle estimation performance.

Figure 6 demonstrates the angle estimation performance comparison with different L, where we compare our algorithm with RD-Capon and RD-ESPRIT algorithms. As shown in Figure 6 that the proposed algorithm acquires better angle estimation performance compared with the RD-ESPRIT and RD-Capon algorithms, especially for the finite snapshot case. According to Figure 6, the angle estimation performance of our technique is enhanced with L increasing.

Figure 7 describes the angle estimation performance comparison of our technique for different transmitting and receiving antennas, respectively. It is manifested that from Figure 7 that angle estimation error will be reduced with the increase of number of

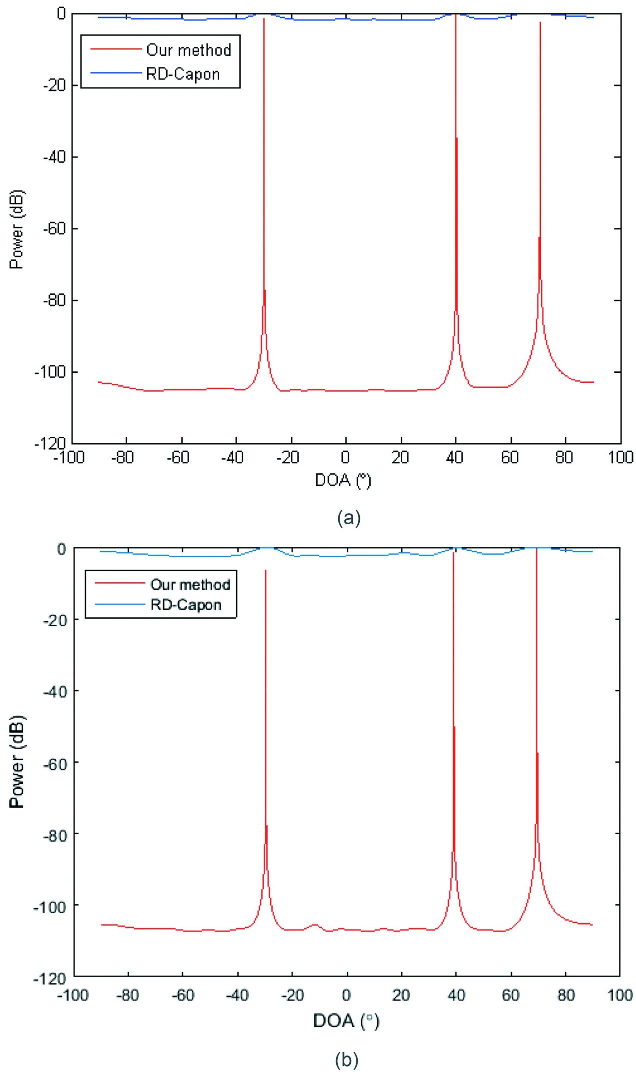

Figure 3. (a) Spatial spectra comparison for three coherent targets. DOAs: $30^\circ, 40^\circ, 70^\circ$ and $L = 300$. (b) Spatial spectra comparison of three coherent targets. DOAs: $30^\circ, 40^\circ, 70^\circ$ and $L = 200$.

antennas. Multiple transmitting/receiving antennas boost angle estimation performance owing to the diversity gain.

In this simulation, we demonstrate the biases against angular separation between two correlated signals with a correlation coefficient of 0.9, and θ_2 is held fixed at -3°, $\theta_1 = \theta_2 + \Delta\theta$ where $\Delta\theta$ varies from 1° to 20° with 1° interval with $M = N = 8$, $L = 100$ and SNR = 10 dB. The points on each curve are obtained by an average over 100 experiments. As we have seen from Figure 8, we can find it that our technique can resolve closely spaced correlated sources without any decorrelation operation and has smaller biases, especially when correlated sources are more than about 3° apart, the estimation bias of our technique vanishes. In other words, our technique has beneficial angle estimation performance.

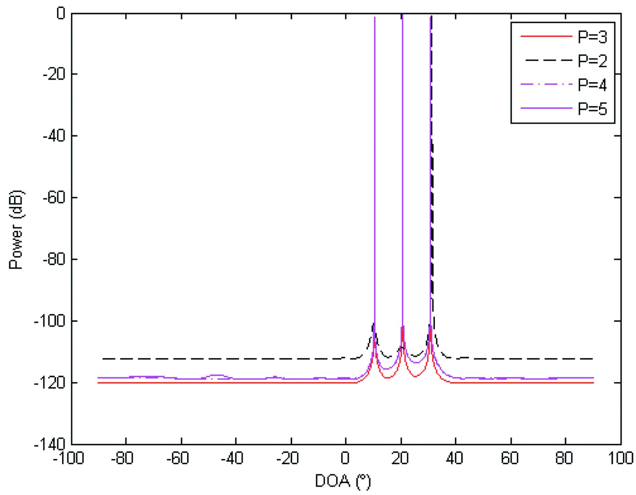

Figure 4. Sensitivity of the proposed algorithm for target priori information. The correct number is 3.

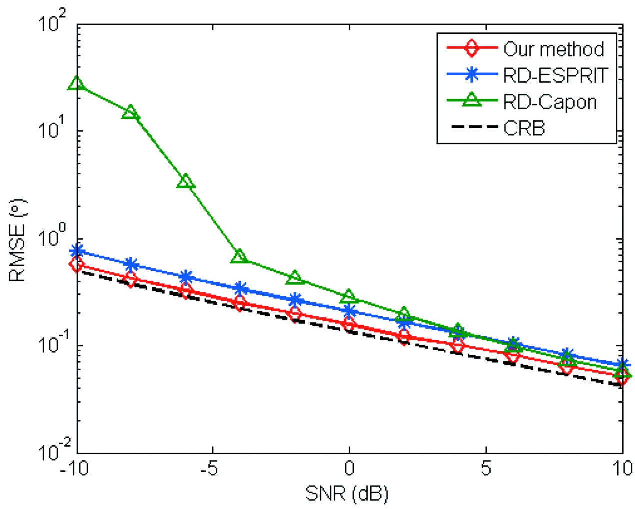

Figure 5. Angle estimation performance comparison with three uncorrelated targets. $M = N = 6, L = 200$.

6. Conclusion

This paper has focused on the DOA estimation problem in monostatic MIMO radar. The success of the proposed algorithm lies in: i) constructing a new real-valued double weighted $l_{2,1}$-norm minimisation model; ii) deriving an improved reduced-dimension technique; and iii) designing the optimal and sparse weights carefully. All these new schemes enable the proposed method to work well in the cases of few snapshots, low signal-to-noise ratio (SNR), closely spaced targets, or strongly correlated sources. Numerical simulations further prove the effectiveness of the proposed method.

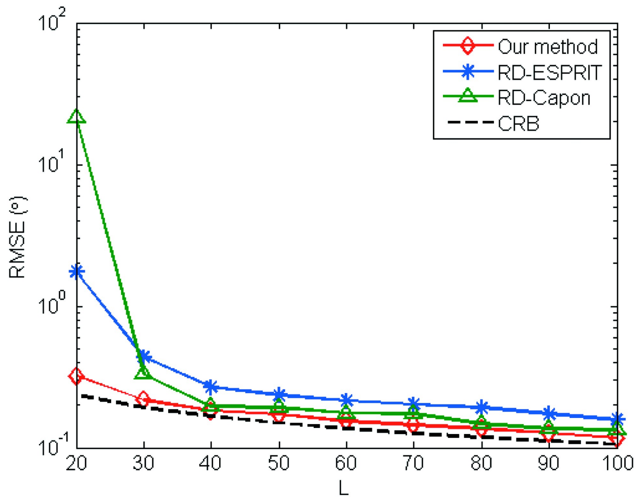

Figure 6. Angle estimation performance comparison with different L. $M = N = 6$, SNR = 5 dB.

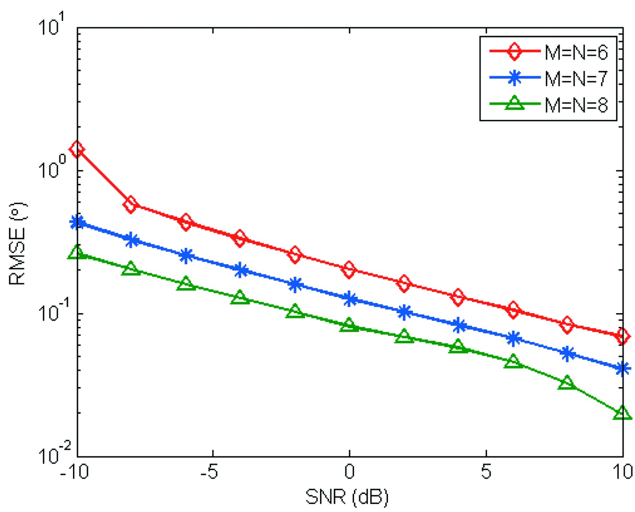

Figure 7. Angle estimation performance comparison with different M and N. $L = 100$.

Authors' contributions

Bao contributed to the design of the study. Bao designed and implemented the proposed method as well as performed the experiments. Bao drafted the manuscript with the guidance of Prof. Zhang and Prof. Ercan. Prof. Gini and Prof. Tao gave some beneficial advices to the work. Dr Lei contributed to amplitude error calibration method by our discussion, and provide part of codes. He and his collaborators applied it to their unitary sparse Bayesian learning method. All authors read and approved the final manuscript.

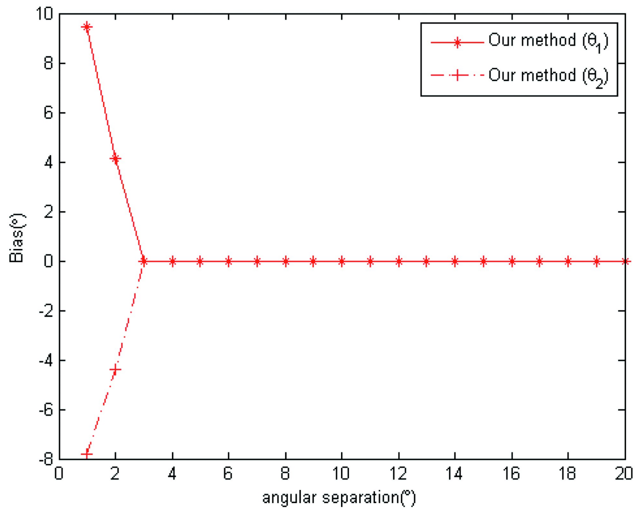

Figure 8. Bias of DOA estimation versus angular separation.

Disclosure statement

No potential conflict of interest was reported by the authors.

Funding

This work was supported by the Natural Science Foundation of China under Grants 61571341, 61201312, 91530113; the Fundamental Research Funds for the Central Universities of China (Nos. BDY171416 and JB140306); the Natural Science Foundation of Shaanxi Province in China (2015JM6275); and the Doctor Research Foundation (107020313).

References

Chen, D., Chen, B., & Qian, G. (2008). Angle estimation using ESPRIT in MIMO radar. *Electronics Letters*, *44*(12), 770–771.

Chen, J., Gu, H., & Su, W. (2008). Angle estimation using ESPRIT without pairing in MIMO radar. *Electronics Letters*, *44*(24), 1422–1423.

Gao, X., Zhang, X., Feng, G., Wang, Z., & Xu, D. (2009). *On the MUSIC-derived approaches of angle estimation for bistatic MIMO radar*. In *Proc: Int'l Conf. Wireless Networks and Inf. Syst* ,Shanghai, China,(pp. 343–346).

Grant, M., & Boyd, S. (2012). CVX: MATLAB software for disciplined convex programming, version 1.22.

Haardt, M., & Nossek, J. (1995). Unitary esprit: How to obtain increased estimation accuracy with a reduced computational burden. *IEEE Transactions on Signal Processing*, *43*, 1232–1242.

Haimovich, A. M., Blum, R., & Cimini, L. J. (2008). MIMO radar with widely separated antennas. *IEEE Signal Processing Magazine*, *25*(1), 116–129.

Haimovich, E. A., Blum, R., Chizhik, D., Ciminim, L., & Valenzuela, R. (2004, April 26–29). *MIMO radar: An idea whose time has come*. *Proceedings of the IEEE radar conference*, Philadelphia (pp.71–78). PA, USA.

Harry, V. T. (2002). *Optimum array processing, part IV of detection, estimation, and modulation theory*. Wiley-Interscience, ISBN 0-471-09390-4.

Hassanien, A., & Vorobyov, S. A. (2011). Transmit energy focusing for DOA estimation in MIMO radar with colocated antennas. *IEEE Transactions on Signal Processing*, *59*(6), 2669–2682.
Hu, N., Ye, Z. F., Xu, D. Y., & Cao, S. H. (2012). A sparse recovery algorithm for DOA estimation using weighted subspace fitting. *Signal Processing*, *92*, 2566–2570.
Huarng, K., & Yeh, C. (1991). A unitary transformation method for angle-of-arrival estimation. *IEEE Transactions on Signal Processing*, *39*, 957–977.
Hyder, E. J., & Mahata, K. (2008). Enhancing sparsity by reweighted l_1 minization. *Journal of Fourier Analysis and Applications*, *14*(5), 877–905.
Li, J., & Li, J. (2012). Reduced-complexity Capon for direction of arrival estimation in a monostatic multiple-input multiple-output radar. *IET Radar, Sonar & Navigation*, *8*(8), 796–801.
Li, J., & Stoic, P. (2007). MIMO radar with colocated antennas. *IEEE Signal Processing Magazine*, *24*(5), 106–114.
Liu, Z. M., Huang, Z. T., & Zhou, Y. Y. (2013). Array signal processing via sparsity-incuding representation of the array covariance matrix. *IEEE Transactions on Aerospace and Electronic Systems*, *49*(3), 1710–1724.
Malioutov, D., Cetin, M., & Willsky, A. S. (2005). A sparse signal reconstruction perspective for source localization with sensor arrays. *IEEE Transactions on Signal Processing*, *53*(8), 3010–3022.
Qian, J. H., He, Z. S., & Zhang, W. (2018). Robust adaptive beamforming for multiple-input multiple-output radar with spatial filtering techniques. *Signal Processing*, *143*, 152–160.
Steffens, C., & Pesavento, M. (2018). Block and rank-sparse recovery for direction finding in partly calibrated arrays. *IEEE Transactions on Signal Processing*, *66*(2), 384–399.
Stoica, P., & Nehorai, A. (1990). Performance study of conditional and unconditional direction-of-arrival estimation. *IEEE Transactions on Acoustics, Speech, and Signal Processing*, *38*, 1783–1795.
Thakre, A., Haardt, M., & Giridhar, K. (2009). Single snapshot spatial smoothing with improved effective array aperture. *IEEE Signal Processing Letters*, *16*, 505–508.
Viberg, M., & Ottersten, B. (1991). Sensor array processing based on subspace fitting. *IEEE Transactions on Signal Processing*, *39*(5), 1110–1121.
Viberg, M., Ottersten, B., & Kailath, T. (1991). Detection and estimation in sensor arrays using weighted subspace fitting. *IEEE Transactions on Signal Processing*, *39*(11), 2436–2449.
Wang, J., Huang, Z. T., & Zhang, Y. Y. (2011). Direction-of-estimation based on joint sparsity. *Sensors*, *11*, 9098–9108.
Xie, R., Liu, Z., & Zhang, Z. J. (2010). DOA estimation for monostatic MIMO radar using polynomial rooting. *Signal Processing*, *90*, 3284–3288.
Xu, L., Li, J., & Stocia, P. (2006). *Atapitve technique for MIMO radar*, *Proceedings of the 4th IEEE Workshop on Sensor Array and Multi-Channel Processing* (pp. 258–262). Waltham, MA.
Yin, J. H., & Chen, T. Q. (2011). Direction-of-arrival estimation using a sparse representation of array covariance vectors. *IEEE Transactions on Signal Processing*, *59*(9), 4489–4493.
Zhang, X., & Xu, D. (2011). Low-complexity ESPRIT-Based DOA estimation for colocated MIMO radar using reduced-dimension transformation. *Electronics Letters*, *47*(4), 283–284.
Zhen, C. D., Li, G., Liu, Y., & Wang, X. Q. (2012). Subspace weighted $l_{2,\,1}$ minimization for sparse signal recovery. *EURASIP Journal on Advances in Signal Processing*, *98*, 1–11.
Zheng, C. D., Li, G., & Wang, X. Q. (2013). Combination of weighted $l_{2,\,1}$ minimization with unitary transformation for DOA estimation. *Signal Processing*, *93*, 3430–3434.